

Cite this: *J. Mater. Chem. C*, 2020, **8**, 11540

Supramolecular oligourethane gel as a highly selective fluorescent “on–off–on” sensor for ions†

Yulin Feng,^{‡a} Nan Jiang,^{‡a} Dongxia Zhu,^{id} *^a Zhongmin Su,^{id} *^a and Martin R. Bryce,^{id} *^b

Stimuli-responsive supramolecular gels (SRSGs) are an important class of smart materials. It is of practical importance to develop an SRSG which can both detect and remove toxic metal ions. We have designed and synthesized an aggregation induced emission (AIE)-active oligourethane (OU) gelator which self-assembles into a supramolecular gel (OUG), through hydrogen-bonding, π - π stacking and van der Waals interactions. By taking advantage of the weak and dynamic nature of these non-covalent bonds, OUG shows stimuli-response to multiple factors. Importantly, OUG has the capacity for real-time detection and high selectivity for Fe^{3+} , HSO_4^- and F^- . The lowest detection limits are in the range of 5.89×10^{-9} to 8.17×10^{-8} M, indicating high sensitivity. More importantly, OUG is shown to adsorb and separate Fe^{3+} from aqueous solution, with an absorbing rate of up to 97.5%. A simple writing board was fabricated, which could be written repeatedly and reused. OUG acts as a reversible and recyclable “on–off–on” fluorescence sensor via competitive cation- π and cation-anion interactions. OUG has great potential as an environmentally sustainable probe for ions.

Received 18th May 2020,
Accepted 16th July 2020

DOI: 10.1039/d0tc02381g

rsc.li/materials-c

Introduction

Stimuli-responsive supramolecular gels (SRSGs) have the ability to respond to a chemical substance,¹ light,² heat,³ pH⁴ or pressure.⁵ They have been applied in chemical sensors,⁶ displays,⁷ drug deliveries⁸ and other fields.⁹ Responsive behavior can be achieved by a gel–sol state transition or by changing the luminescence.^{7,10} The latter response works by changing the gel's fluorescence intensity or color, and can be free from the influence of temperature,² pH,¹¹ an oxidizing agent,⁸ and other factors.¹² Therefore luminescence detection has considerably higher sensitivity and more reliable real-time response.^{13–15} Traditional conjugated gelators usually suffer from aggregation-caused quenching (ACQ), which sharply weakens the emission behavior in aggregation or solid states, thereby limiting their applications.¹⁶ The emergence of polymers/oligomers with aggregation-induced emission (AIE) properties has been a

breakthrough in the field.^{17,18} In addition to their excellent emission characteristics, AIE-active supramolecular gels show strong absorption activity and synergistic effects because of their large contact area with analytes.¹⁹

Recently, our group has explored AIE-active poly/oligourethane-based unconventional luminophores, which are without typical polycyclic π -conjugated units. These materials show obvious advantages like environmental friendliness, excellent hydrophilicity, chain flexibility, ease of synthesis and structural versatility compared with traditional organic luminescent materials.^{20–22}

Fe^{3+} is an indispensable element in the process of oxygen uptake and metabolism.²³ However, an excess of Fe^{3+} might cause pathological diseases like cancer and organ dysfunction.²⁴ F^- and HSO_4^- also play essential roles in human biological processes,^{25,26} although undue fluoride may cause kidney problems, dental and skeletal fluorosis.²⁷ HSO_4^- can produce poisonous SO_4^{2-} under acidic conditions, which will stimulate the skin and eyes and can even cause respiratory paralysis.²⁸ Thus, methods to efficiently detect these ions have received extensive attention. The established detection techniques, such as inductively coupled plasma spectroscopy,²⁹ high performance liquid chromatography (HPLC)³⁰ and electrochemical methods,³¹ all require tedious sample preparations, sophisticated instruments and professional operators. However, fluorescent sensor molecules, which convert and amplify the signals into a visible

^a Key Laboratory of Nanobiosensing and Nanobioanalysis at Universities of Jilin Province, Department of Chemistry, Northeast Normal University, 5268 Renmin Street, Changchun, Jilin Province 130024, P. R. China.
E-mail: zhudx047@nenu.edu.cn, zmsu@nenu.edu.cn

^b Department of Chemistry, Durham University, Durham, DH1 3LE, UK.
E-mail: m.r.bryce@durham.ac.uk

† Electronic supplementary information (ESI) available: ¹H NMR spectra and photophysical properties. See DOI: 10.1039/d0tc02381g

‡ These authors contributed equally to the preparation of this work.



and easily recognized fluorescent output, offer a more significant practical method.^{6,32}

Herein, we report an AIE-active supramolecular oligourethane gel (**OUG**) and demonstrate its usage as a specific Fe³⁺ sensor in an aqueous environment. The material is based on the following design criteria: (i) inserting benzophenone into an oligourethane (OU) backbone provides C=O units with prominent hydrogen-bonding sites for self-assembly, and formation of oxygen clusters, which could enhance fluorescent emission.³³ (ii) Inserting linear 1,6-diisocyanatohexane offers strong van der Waals interactions among alkyl chains, limiting internal rotation of the molecular chains, thereby blocking the non-radiative pathways and favoring AIE. Taking advantage of the rich hydrogen bond acceptors/donors (C=O/N-H) among the oligourethane skeleton,^{34–41} we introduced solvents with hydrogen-bonding acceptor units (C=O or S=O) as external crosslinking agents, to self-assemble a supramolecular oligourethane gel (**OUG**) relying on multiple hydrogen bonds.

Results and discussion

Synthesis and characterization

The OU was synthesized through a facile procedure as shown in Scheme S1 (ESI[†]), by the reaction of 4,4'-dihydroxybenzophenone, hexamethylene diisocyanate and DABCO in anhydrous tetrahydrofuran and end-capping with polyethylene glycol monomethyl ether to give a viscous solution. The product was purified by a counter precipitation method. ¹H NMR and FTIR characterization data are given in Fig. 1a and in the ESI[†], confirming the structure of OU. The *M_n* value of 1814 g mol⁻¹, calculated from the

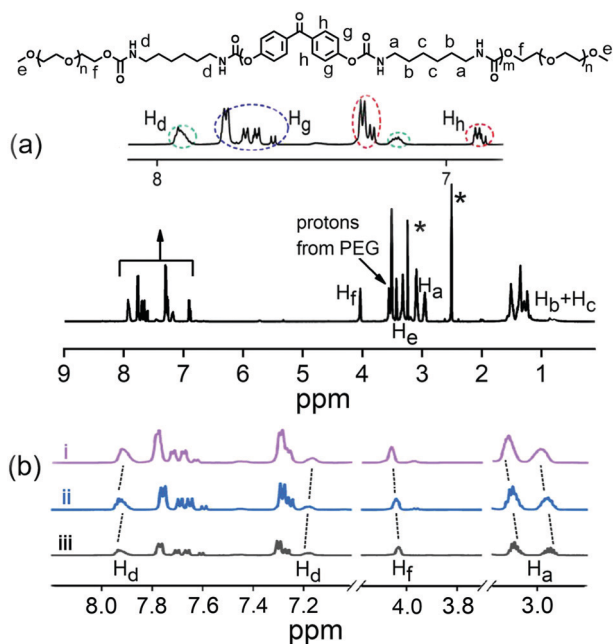


Fig. 1 (a) ¹H NMR spectrum of OU in DMSO-*d*₆ (* indicates peaks from the solvent and water); H-atom labeling is shown on the structure of OU. (b) The partial ¹H NMR spectra of OU in DMSO-*d*₆ at different concentrations: (i) 0.925 mM, (ii) 3.7 mM, and (iii) 25.0 mM.

¹H NMR data, established that OU should be classified as an oligomer.⁴² The FTIR spectra (Fig. S1, ESI[†]) showed absorbance bands at 3323 cm⁻¹ and 1706 cm⁻¹, assigned to stretching vibrations of N-H and C=O, indicating the formation of amide bonds. Absorbance bands at 2936 cm⁻¹ and 2860 cm⁻¹ correspond to ν(-CH₂-) and at 1163 cm⁻¹ correspond to ν(C-O-C) stretching vibrations. The UV-Vis absorption spectrum of OU in the solid-state (Fig. S2, ESI[†]) showed a major peak at 277 nm from a π-π* transition of the aromatic rings.⁴³

Self-assembly gelation

OU spontaneously self-assembles in certain solvents (notably dimethyl formamide and dimethylsulfoxide) transforming into a supramolecular gel (Table S1, ESI[†]). The lowest critical gelation concentration (CGC) of OU is 4% (w/v, 10 mg mL⁻¹ = 1%), and the corresponding gel-sol transition temperature (*T_{gel}*) is 85–87 °C. In order to gain an insight into the self-assembly mechanism, ¹H NMR, FTIR, XRD and urea addition experiments were conducted. ¹H NMR spectra were recorded for different concentrations of OU in DMSO-*d*₆ (Fig. 1b). The H_a and H_f proton signals are shifted *ca.* 0.04 and 0.03 ppm upfield compared to pure **OUG** upon adding 25 mM Fe³⁺. Meanwhile, the signals of protons H_d (the NH groups) shifted slightly downfield *ca.* 0.01 ppm.⁴⁴ These results confirmed the H-bonding interactions between amide groups and van der Waals interactions between alkyl chains. Comparing the FTIR data before and after gelation (Fig. S1, ESI[†]), the N-H stretching absorbance bands of **OUG** are broader and move to significantly higher wavenumbers (3323 to 3361 cm⁻¹) in the solid state compared to the gel state: these data suggest hydrogen bonds play a critical role in the gelation process.^{45,46}

It is well known that adding urea, which has a high propensity to form hydrogen bonds, can disrupt existing hydrogen bonds in a supramolecular structure.^{47,48} Accordingly, adding urea (10 equiv.) into **OUG** and heating the gel, led to the formation of a sol. It was observed that after adding urea, the sol did not revert back to gel, even when the **OUG**-urea mixture was cooled at 15 °C for several days, indicating that the gelation is driven by hydrogen bonds among OU molecular chains (Fig. 2a). Besides, the X-ray diffraction (XRD) peaks of **OUG**

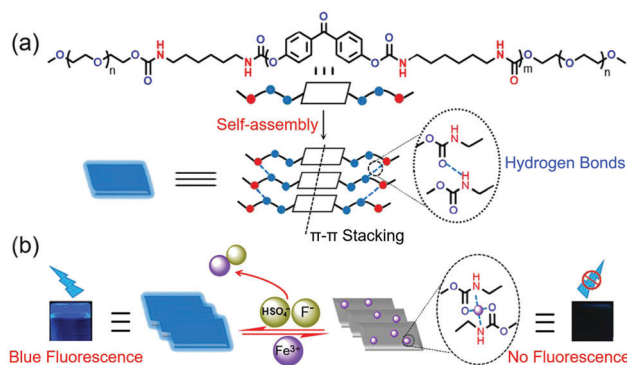


Fig. 2 (a) Structure of OU and its self-assembly gelation process. (b) Schematic diagram for the ion sensing processes of **OUG**.



$2\theta = 20.54^\circ, 23.22^\circ$ corresponding to d -spacings of 4.32 Å and 3.83 Å, respectively, also indicated the presence of π - π stacking interactions (Fig. S11b, ESI†), further promoting the self-assembly behavior. **OUG** showed weak fluorescence in the sol state, however, after transforming to the gel state, the emission intensity of **OUG** at 439 nm increased 6 times (Fig. S3, ESI†), indicating that **OU** is an AIE-active gelator.⁴⁹

Stimuli-responsive behaviors

OUG exhibits a high selectivity to Fe^{3+} over other metal ions. By monitoring the change of fluorescence, we investigated the recognition characteristics of **OUG** towards metal ions. Using nitrate salts as the cation sources, an aqueous metal ion solution of $\text{Na}^+, \text{Ca}^{2+}, \text{Co}^{2+}, \text{Cu}^{2+}, \text{Mn}^{2+}, \text{Ni}^{2+}, \text{Cr}^{3+}, \text{La}^{3+}, \text{Fe}^{3+}, \text{Sr}^{2+}, \text{Ce}^{3+}, \text{Ag}^+, \text{Al}^{3+}, \text{Mg}^{2+}, \text{Cd}^{2+}, \text{Pb}^{2+}$ or Fe^{2+} ($c = 0.2 \text{ M}$) was added to the **OUG** to generate the corresponding metal-gels.^{50–53} As shown in Fig. 3a and c, initially, the **OUG** had a strong blue fluorescence emission. When different metal ions were added, only Fe^{3+} quenched the fluorescence of **OUG**. Thus, the **OUG** could effectively and selectively detect Fe^{3+} . To further evaluate the sensitivity of **OUG** for Fe^{3+} , the fluorescence behavior of **OUG** was monitored by continuous titrations with Fe^{3+} . As shown in Fig. S5a (ESI†), with the increasing addition of Fe^{3+} (0–1.1 equiv.), the emission intensity of the corresponding metal-gels (**OUG**) at 439 nm gradually decreased. The limit of detection (LOD) of **OUG** towards Fe^{3+} was calculated to be $5.89 \times 10^{-9} \text{ M}$ based on the $3\delta/S$ method⁵⁴ (Fig. S4 and S5a, ESI†), confirming the high selectivity of **OUG** as a sensor for Fe^{3+} compared with other reported sensor

systems (Table S2, ESI†). The high selectivity of **OUG** to Fe^{3+} is attributed to two reasons: firstly, unpaired electrons in Fe^{3+} cause a paramagnetic effect, prompting energy dissipation of excited states through non-radiative pathways.⁵⁵ Secondly, the high ionic strength of Fe^{3+} could easily induce the transfer of π -electrons from the urethane backbone to Fe^{3+} through cation- π interactions.⁵⁶ Both of these effects will cause the fluorescence quenching of **OUG**.

The response of **OUG** towards anions was further investigated, using tetrabutylammonium salts as the anion sources, adding aqueous solutions of anions including $\text{HSO}_4^-, \text{ClO}_4^-, \text{I}^-, \text{CN}^-, \text{PF}_6^-, \text{F}^-, \text{Cl}^-, \text{Br}^-, \text{NO}_3^-, \text{AcO}^-$ ($c = 0.2 \text{ M}$) to **OUG**.^{57–60} As shown in Fig. 3b and c, when HSO_4^- and F^- were added the emission at 439 nm recovered immediately, whereas the other anions did not lead to a comparable fluorescence recovery of **OUG**. These phenomena confirmed the excellent selectivity of **OUG** towards HSO_4^- and F^- . This selectivity is explained by the strong coordinating capacity of HSO_4^- and F^- with Fe^{3+} , in contrast to (metal-free) **OUG**. These two anions could competitively bind to Fe^{3+} in **OUG** and induce the re-emission of **OUG**. Titration experiments evaluated the sensing efficiency of **OUG** to HSO_4^- and F^- . Limit of detection (LOD) values were calculated according to the $3\delta/S$ method to be $8.17 \times 10^{-8} \text{ M}$ for F^- and $1.16 \times 10^{-8} \text{ M}$ for HSO_4^- (Fig. S5b and Fig. S7–S9, ESI†). Notably the LOD values of **OUG** are lower than many other reported F^- and HSO_4^- fluorescence sensors (Table S2, ESI†). The gel **OUG** selectively senses Fe^{3+} , and the metal-gel **OUG** selectively responds to F^- and HSO_4^- . This property makes gel **OUG** and metal-gel **OUG** act as an efficient “on-off-on” fluorescence sensor controlled by Fe^{3+} , HSO_4^- or F^- with excellent reversibility. A simple regeneration treatment verified the recyclability of **OUG**. An anion solution (F^- or HSO_4^- , $2 \times 10^{-5} \text{ mol L}^{-1}$; 10 mL) was added into metal-gel **OUG**, stirring the mixture for 5 min, centrifuging and recycling **OUG** for again detecting ions. As shown in Fig. S10 (ESI†), after five consecutive cycles, the intensity of the **OUG** signal is essentially unchanged, indicating the excellent recyclability and reversibility of the **OUG** for the detection of Fe^{3+} and HSO_4^- or F^- .

Mechanism of cation-anion sensor

When adding aqueous solution of Fe^{3+} into **OUG**, Fe^{3+} can diffuse in the solution. Due to the high ionic strength of Fe^{3+} , the π -electrons in the urethane groups of **OUG** are easily induced to form cation- π interactions quenching the fluorescence. The recognition mechanisms of **OUG** to Fe^{3+} were investigated *via* a combination of ^1H NMR, FTIR, XRD and SEM analysis. In the ^1H NMR titration experiments, with the increasing amount of Fe^{3+} added into **OU**, protons H_d , H_f and H_a all displayed clear upfield shifts (Fig. 4a), indicating that the **OUG** combined with Fe^{3+} *via* cation- π interactions between the urethane groups and Fe^{3+} .^{56,61} As Fig. 4b shows, by adding F^- or HSO_4^- (3.7 mM) into a sample of **OU** (with 2 equiv. Fe^{3+}), all the protons recovered the chemical shifts as in the original **OU**: H_d (from 7.85 to 7.93 ppm and 7.09 to 7.19 ppm), H_f (from 3.94 to 4.03 ppm) and H_a (from 3.01 to 3.09 ppm and 2.87 to

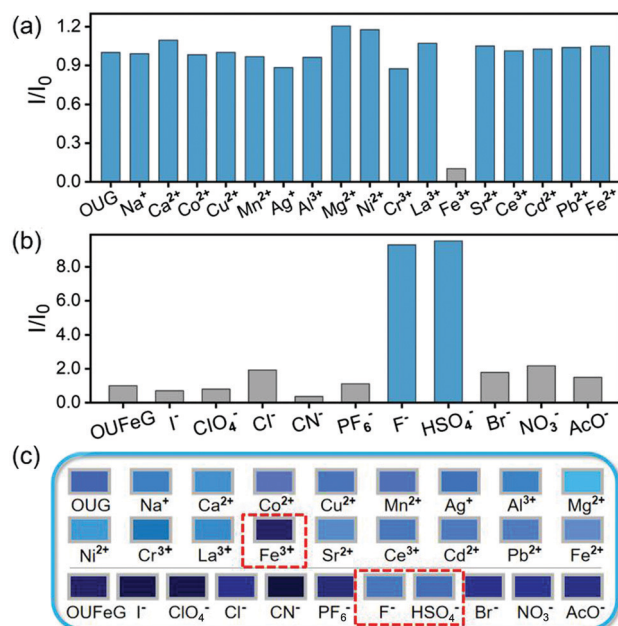


Fig. 3 (a) Fluorescence responses of **OUG** (in DMF, 10% (w/v)) toward Fe^{3+} and other metal ions at room temperature. (b) Fluorescence responses of **OUG** (in DMF, 10% (w/v)) toward F^- , HSO_4^- and other anions at room temperature. All data represent the fluorescence intensity ratio I/I_0 (I and I_0 are the final fluorescence intensity and initial fluorescence intensity for the gel with each ion tested at 384 nm). (c) Photos of **OUG** fluorescence responses to various cations and anions.



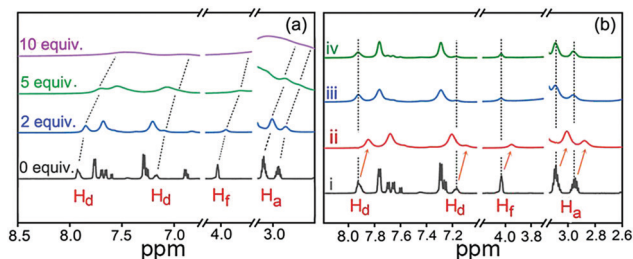


Fig. 4 (a) ^1H NMR titration spectra (298 K) of 0.925 mM OU with various equivalents of Fe^{3+} in $\text{DMSO}-d_6$ solution. (b) ^1H NMR spectra of (i) OU (ii) **OUFeG** (iii) **OUFeG** + HSO_4^- and (iv) **OUFeG** + F^- .

2.95 ppm), which indicated the cation–anion interactions between Fe^{3+} and F^- or HSO_4^- could release the π -electrons of urethane groups, thus recovering the fluorescence of **OUG**.

In the FTIR experiments (Fig. S11a, ESI †), when Fe^{3+} was added into **OUG** to form **OUFeG**, the stretching absorbance bands of N–H, C=O and C–O–C shifted from 3361 cm^{-1} , 1708 cm^{-1} and 1161 cm^{-1} to 3480 cm^{-1} , 1673 cm^{-1} and 1158 cm^{-1} respectively, which further confirmed that Fe^{3+} interacts with π -electrons of the urethane groups, thus influencing H-bonds between the amide groups.^{6,57} After the addition of F^- or HSO_4^- into the **OUFeG**, the C=O, N–H and C–O–C all reverted to their initial positions (Fig. S11a, ESI †). These observations suggested that F^- and HSO_4^- competitively bound to Fe^{3+} rather than to **OUG**. Moreover, the XRD peaks of **OUG** moved with adding Fe^{3+} into **OUG**, and recovered when F^- or HSO_4^- was added into **OUFeG** (Fig. S11b, ESI †).

To get further insight into the mechanism of cation–anion sensing, as shown in Fig. 5, the SEM studies were carried out. Fig. 5a demonstrates that gel **OUG** shows a lamellar stacking structure with a smooth surface. This structure was converted into a honeycomb structure in the metal-gel **OUFeG** (Fig. 5b), while in gel **OUFeG** + HSO_4^- and **OUFeG** + F^- , the image again showed a smooth lamellar stacking structure (Fig. 5c and d). Such morphological change is attributed to the cation– π interactions between **OUG** and Fe^{3+} , breaking hydrogen bonding

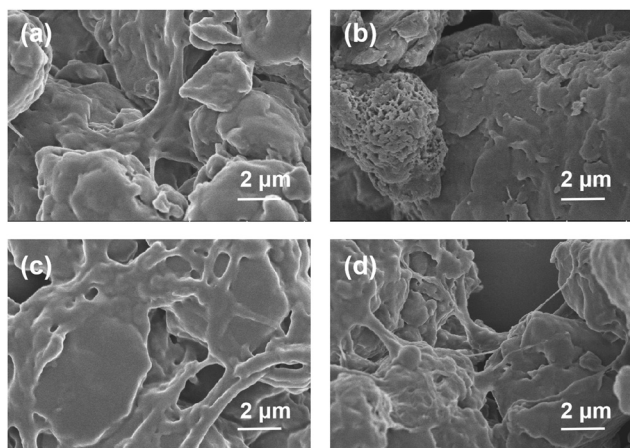


Fig. 5 SEM images of (a) **OUG**; (b) **OUFeG**; (c) **OUFeG** + HSO_4^- ; (d) **OUFeG** + F^- .

between the **OUG** chains and modifying the supramolecular structure.^{57,61} After adding F^- or HSO_4^- into **OUFeG**, π -electrons of **OUG** were released, hydrogen bonds are rebuilt and the morphology is recovered. These experimental results indicated that the fluorescence of **OUG** can be reversibly switched by Fe^{3+} (off) and then by F^- or HSO_4^- (on), through repeated competition between cation– π and cation–anion interactions (Fig. 2b).

Application in the rapid removal of Fe^{3+}

The development of new sorbents for the sensing and extraction of metal ions from environmental and biological samples is of current importance.^{62,63} The performance of **OUG** to effectively remove Fe^{3+} from aqueous solution was analyzed by atomic absorption spectrometry (Table S3, ESI †). Specifically, **OUG** (0.2 g) was added to a dilute aqueous solution of Fe^{3+} ($1 \times 10^{-5}\text{ mol L}^{-1}$ in 10 mL water) and the mixture was stirred for 10 min. The precipitate was separated by centrifuging at 5000 rpm for 5 min and the supernatant was retained, the residual concentration of Fe^{3+} was about $2.5 \times 10^{-7}\text{ mol L}^{-1}$. Experimental results demonstrated that 97.5% of Fe^{3+} could be efficiently removed by **OUG** even from extremely dilute solutions, which indicated the excellent adsorption capacity of **OUG** towards Fe^{3+} .^{6,56,57,64} As shown in Fig. S6 (ESI †), adsorption tests of **OUG** toward Fe^{3+} in the pH range from 4 to 10 showed that the adsorption of **OUG** toward Fe^{3+} showed excellent stability at different pH conditions (in the range of 92.1–97.5%). **OUG** can selectively detect with high-efficiency and rapidly remove toxic Fe^{3+} , offering potential practical applications in combating heavy metal ion pollution and in environmental remediation.

Application as a writing display material

Based on the above-mentioned “on–off–on” properties, the **OUG** has a great potential as a rewritable fluorescent display material. As a proof-of-concept a rewritable board was constructed (Fig. 6). The detailed steps are described as follows: (i) **OUG** sol (10%) was poured onto a clean quartz plate surface and dried under ambient conditions to give a film emitting strong blue fluorescence under ultraviolet radiation (365 nm). (ii) Writing the symbol “Fe” on the film with a brush dipped in

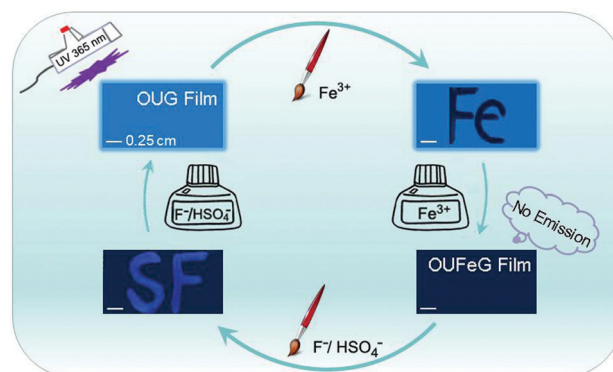


Fig. 6 An erasable writing board of **OUG** based on its ion-controlled fluorescent switching properties.



aqueous Fe^{3+} solution (0.3 M), a dark “Fe” image was clearly displayed due to the fluorescence quenching effect of Fe^{3+} on OUG. (iii) The whole OUG film was transformed into a non-fluorescent display board by brushing with Fe^{3+} solution. (iv) Two new letters “S” and “F” could be written again with the same brushing method using HSO_4^- and F^- solutions (0.3 M), respectively. Visually, the letters emitted blue fluorescence under a UV lamp. Combining these practically very simple processes with the excellent recyclability of OUG (discussed above; Fig. S10, ESI[†]) means that OUG has promising applications as a fluorescent writing display material.

Conclusion

In conclusion, a novel supramolecular AIE gel, OUG, was designed and synthesized by a straightforward “one-pot” procedure. The dynamic and reversible noncovalent interactions endow OUG with distinct advantages of a reversible and highly sensitive response to Fe^{3+} , HSO_4^- , and F^- , acting as an “on-off-on” fluorescent sensor for these cationic and anionic species. Importantly, OUG can absorb up to 97.5% Fe^{3+} from a water environment. This rapid, simple, low cost and highly sensitive material has great potential for practical applications in intelligent sensing, handling heavy metal ion pollution and environmental remediation.

Conflicts of interest

There are no conflicts to declare.

Acknowledgements

The work was funded by NSFC (No. 51473028), the key scientific and technological project of Jilin province (20150204011GX, 20160307016GX, 20190701010GH), the Development and Reform Commission of Jilin province (20160058, 2020C035-5), Open Project of State Key Laboratory of Supramolecular Structure and Materials (sklssm202039). M. R. B. thanks EPSRC grant EL/L02621X/1 for funding.

Notes and references

- L.-J. Chen, G.-Z. Zhao, B. Jiang, B. Sun, M. Wang, L. Xu, J. He, Z. Abliz, H. Tan, X. Li and H.-B. Yang, *J. Am. Chem. Soc.*, 2014, **136**, 5993–6001.
- S.-H. Hsiao and S.-h. Hsu, *ACS Appl. Mater. Interfaces*, 2018, **10**, 29273–29287.
- J. B. Beck and S. J. Rowan, *J. Am. Chem. Soc.*, 2003, **125**, 13922–13923.
- M. Zhang, D. Xu, X. Yan, J. Chen, S. Dong, B. Zheng and F. Huang, *Angew. Chem. Int. Ed.*, 2012, **51**, 7011–7015.
- J. Lai, H. Zhou, Z. Jin, S. Li, H. Liu, X. Jin, C. Luo, A. Ma and W. Chen, *ACS Appl. Mater. Interfaces*, 2019, **11**, 26412–26420.
- Y.-M. Zhang, W. Zhu, W.-J. Qu, K.-P. Zhong, X.-P. Chen, H. Yao, T.-B. Wei and Q. Lin, *Chem. Commun.*, 2018, **54**, 4549–4552.
- Q. Lin, B. Sun, Q.-P. Yang, Y.-P. Fu, X. Zhu, Y.-M. Zhang and T.-B. Wei, *Chem. Commun.*, 2014, **50**, 10669–10671.
- X. Cheng, Y. Jin, T. Sun, R. Qi, H. Li and W. Fan, *Colloids Surf., B*, 2016, **141**, 44–52.
- M. Ikeda, T. Tanida, T. Yoshii, K. Kurotani, S. Onogi, K. Urayama and I. Hamachi, *Nat. Chem.*, 2014, **6**, 511–518.
- Z.-Y. Li, Y. Zhang, C.-W. Zhang, L.-J. Chen, C. Wang, H. Tan, Y. Yu, X. Li and H.-B. Yang, *J. Am. Chem. Soc.*, 2014, **136**, 8577–8589.
- K. Manokruang and D. S. Lee, *Macromol. Biosci.*, 2013, **13**, 1195–1203.
- T. Tanaka, *Phys. Rev. Lett.*, 1978, **40**, 820–823.
- Y. Chang, J. Fu, K. Yao, B. Li, K. Xu and X. Pang, *Dyes Pigm.*, 2019, **161**, 331–340.
- B.-J. Wang, W.-K. Dong, Y. Zhang and S. F. Akogun, *Sens. Actuators, B*, 2017, **247**, 254–264.
- X. Liu, T. Chen, F. Yu, Y. Shang, X. Meng and Z.-R. Chen, *Macromolecules*, 2020, **53**, 1224–1232.
- C.-W. Zhang, B. Ou, S.-T. Jiang, G.-Q. Yin, L.-J. Chen, L. Xu, X. Li and H.-B. Yang, *Polym. Chem.*, 2018, **9**, 2021–2030.
- P. Q. Nhien, W.-L. Chou, T. T. K. Cuc, T. M. Khang, C.-H. Wu, N. Thirumalaivasan, B. T. B. Hue, J. I. Wu, S. P. Wu and H.-C. Lin, *ACS Appl. Mater. Interfaces*, 2020, **12**, 10959–10972.
- Y. Bao, E. Guégain, V. Nicolas and J. Nicolas, *Chem. Commun.*, 2017, **53**, 4489.
- R. Hu, A. Qin and B. Z. Tang, *Prog. Polym. Sci.*, 2020, **100**, 101176.
- N. Jiang, G.-F. Li, B.-H. Zhang, D.-X. Zhu, Z.-M. Su and M. R. Bryce, *Macromolecules*, 2018, **51**, 4178–4184.
- N. Jiang, G. Li, W. Che, D. Zhu, Z. Su and M. R. Bryce, *J. Mater. Chem. C*, 2018, **6**, 11287–11291.
- N. Jiang, D. Zhu, Z. Su and M. R. Bryce, *J. Mater. Chem. C*, 2020, **8**, 5137–5142.
- K. P. Carter, A. M. Young and A. E. Plamer, *Chem. Rev.*, 2014, **114**, 4564–4601.
- Y. Fang, J. Tan, H. Choi, S. Lim and D.-H. Kim, *Sens. Actuators, B*, 2018, **259**, 155–161.
- Y. Li, Y. Duan, J. Zheng, J. Li, W. Zhao, S. Yang and R. Yang, *Anal. Chem.*, 2013, **85**, 11456–11463.
- U. Haldar and H.-i. Lee, *Polym. Chem.*, 2018, **9**, 4882–4890.
- L. Li, Y. Ji and X. Tang, *Anal. Chem.*, 2014, **86**, 10006–10009.
- H. J. Kim, S. Bhuniya, R. K. Mahajan, R. Puri, H. Liu, K. C. Ko, J. Y. Lee and J. S. Kim, *Chem. Commun.*, 2009, 7128–7130.
- M. Türkmen, A. Türkmen, Y. Tepe, Y. Töre and A. Ateş, *Food Chem.*, 2009, **113**, 233–237.
- V. Fernández and G. Winkelmann, *Biometals*, 2005, **18**, 53–62.
- B. Bansod, T. Kumar, R. Thakur, S. Rana and I. Singh, *Biosens. Bioelectron.*, 2017, **94**, 443–455.
- X.-Y. Xu and B. Yan, *ACS Appl. Mater. Interfaces*, 2015, **7**, 721–729.



- 33 Q. Zhou, B. Cao, C. Zhu, S. Xu, Y. Gong, W. Z. Yuan and Y. Zhang, *Small*, 2016, **12**, 6586–6592.
- 34 D. Zhang, Y. Zhang, Y. Fan, M.-N. Rager, V. Guérineau, L. Bouteiller, M.-H. Li and C. M. Thomas, *Macromolecules*, 2019, **52**, 2719–2724.
- 35 K. A. Houton, G. M. Burslem and A. J. Wilson, *Chem. Sci.*, 2015, **6**, 2382–2388.
- 36 S. Sami, E. Yildirim, M. Yurtsever, E. Yurtsever, E. Yilgor, I. Yilgor and G. L. Wilkes, *Polymer*, 2014, **55**, 4563–4576.
- 37 D. H. Merino, A. T. Slark, H. M. Colquhoun, W. Hayes and I. W. Hamley, *Polym. Chem.*, 2010, **1**, 1263–1271.
- 38 P. J. Woodward, D. H. Merino, B. W. Greenland, I. W. Hamley, Z. Light, A. T. Slark and W. Hayes, *Macromolecules*, 2010, **43**, 2512–2517.
- 39 D. Hermida-Merino, G. E. Newby, I. W. Hamley, W. Hayes and A. Slark, *Soft Matter*, 2015, **11**, 5799–5803.
- 40 T. S. Babra, M. Wood, J. S. Godleman, S. Salimi, C. Warriner, N. Bazin, C. R. Siviour, I. W. Hamley, W. Hayes and B. W. Greenland, *Eur. Polym. J.*, 2019, **119**, 260–271.
- 41 J. P. Sheth, D. B. Klinedinst, G. L. Wilkes, I. Yilgor and E. Yilgor, *Polymer*, 2005, **46**, 7317–7322.
- 42 T. Mondal, J. Sarkar and S. Ghosh, *Chem. – Eur. J.*, 2016, **22**, 10930–10936.
- 43 Q. Wan, M. Liu, L. Mao, R. Jiang, D. Xu, H. Huang, Y. Dai, F. Deng, X. Zhang and Y. Wei, *Mater. Sci. Eng., C*, 2017, **72**, 352–358.
- 44 J. A. Sáez, B. Escuder and J. F. Miravet, *Chem. Commun.*, 2010, **46**, 7996–7998.
- 45 P. Maiti, G. Radhakrishnan, P. Aruna and G. Ghosh, *Macromol. Symp.*, 2006, **241**, 51–59.
- 46 M.-T. Leiendecker, C. J. Licht, J. Borghs, D. J. Mooney, M. Zimmermann and A. Böker, *Macromol. Rapid Commun.*, 2018, **39**, 1700711.
- 47 M. R. Molla and S. Ghosh, *Chem. – Eur. J.*, 2012, **18**, 9860–9869.
- 48 D. R. Canchi, D. Paschek and A. E. García, *J. Am. Chem. Soc.*, 2010, **132**, 2338–2344.
- 49 X.-M. Jiang, X.-J. Huang, S.-S. Song, X.-Q. Ma, Y.-M. Zhang, H. Yao, T.-B. Wei and Q. Lin, *Polym. Chem.*, 2018, **9**, 4625–4630.
- 50 Q. Lin, X.-M. Jiang, X.-Q. Ma, J. Liu, H. Yao, Y.-M. Zhang and T.-B. Wei, *Sens. Actuators, B*, 2018, **272**, 139–145.
- 51 W. Dong, H. Wu, M. Chen, Y. Shi, J. Sun, A. Qin and B. Z. Tang, *Polym. Chem.*, 2016, **7**, 5835–5839.
- 52 G. Yang, H. Zhang, Y. Wang, X. Liu, Z. Luo and J. Yao, *Sens. Actuators, B*, 2017, **251**, 773–780.
- 53 Q. Lin, B. Sun, Q.-P. Yang, Y.-P. Fu, X. Zhu, T.-B. Wei and Y.-M. Zhang, *Chem. – Eur. J.*, 2014, **20**, 11457–11462.
- 54 D. Dai, Z. Li, J. Yang, C. Wang, J.-R. Wu, Y. Wang, D. Zhang and Y.-W. Yang, *J. Am. Chem. Soc.*, 2019, **141**, 4756–4763.
- 55 S. K. Sahoo, D. Sharma, R. K. Bera, G. Crisponi and J. F. Callan, *Chem. Soc. Rev.*, 2012, **41**, 7195–7227.
- 56 Y.-M. Zhang, W. Zhu, X.-J. Huang, W.-J. Qu, J.-X. He, H. Fang, H. Yao, T.-B. Wei and Q. Lin, *ACS Sustainable Chem. Eng.*, 2018, **6**, 16597–16606.
- 57 Y.-M. Zhang, J.-X. He, W. Zhu, Y.-F. Li, H. Fang, H. Yao, T.-B. Wei and Q. Lin, *Mater. Sci. Eng., C*, 2019, **100**, 62–69.
- 58 H. Xie, F. Zeng, C. Yu and S. Wu, *Polym. Chem.*, 2013, **4**, 5416–5424.
- 59 H. Wan, P. Gu, F. Zhou, H. Wang, J. Jiang, D. Chen, Q. Xu and J. Lu, *Polym. Chem.*, 2018, **9**, 3893–3899.
- 60 G. G. V. Kumar, M. P. Kesavan, G. Sivaraman and J. Rajesh, *Sens. Actuators, B*, 2018, **255**, 3194–3206.
- 61 Q. Lin, P.-P. Mao, Y.-Q. Fan, L. Liu, J. Liu, Y.-M. Zhang, H. Yao and T.-B. Wei, *Soft Matter*, 2017, **13**, 7085–7089.
- 62 W. A. Wan Ibrahim, L. I. Abd Ali, A. Sulaiman, M. M. Sanagi and H. Y. Aboul-Enein, *Crit. Rev. Anal. Chem.*, 2014, **44**, 233–254.
- 63 M. Kataria, M. Kumar and V. Bhalla, *J. Indian Chem. Soc.*, 2018, **95**, 1559–1577.
- 64 J. Liu, Y.-Q. Fan, S.-S. Song, G.-F. Gong, J. Wang, X.-W. Guan, H. Yao, Y.-M. Zhang, T.-B. Wei and Q. Lin, *ACS Sustainable Chem. Eng.*, 2019, **7**, 11999–12007.

